INVITED PAPER

Driver Modeling Based on Driving Behavior and Its Evaluation in Driver Identification

Analysis of car-pedal use and car-following habits may allow the help offered by intelligent driver assistance systems to be customized for individual drivers.

By Chiyomi Miyajima, *Member IEEE*, Yoshihiro Nishiwaki, Koji Ozawa, Toshihiro Wakita, Katsunobu Itou, Kazuya Takeda, *Member IEEE*, and Fumitada Itakura, *Fellow IEEE*

ABSTRACT | All drivers have habits behind the wheel. Different drivers vary in how they hit the gas and brake pedals, how they turn the steering wheel, and how much following distance they keep to follow a vehicle safely and comfortably. In this paper, we model such driving behaviors as car-following and pedal operation patterns. The relationship between following distance and velocity mapped into a two-dimensional space is modeled for each driver with an optimal velocity model approximated by a nonlinear function or with a statistical method of a Gaussian mixture model (GMM). Pedal operation patterns are also modeled with GMMs that represent the distributions of raw pedal operation signals or spectral features extracted through spectral analysis of the raw pedal operation signals. The driver models are evaluated in driver identification experiments using driving signals collected in a driving simulator and in a real vehicle. Experimental results show that the driver model based on the spectral features of pedal operation signals efficiently models driver individual differences and achieves an identification rate of 76.8% for a field test with 276 drivers, resulting in a relative error reduction of 55% over driver models that use raw pedal operation signals without spectral analysis.

KEYWORDS | Car-following; driver identification; driver modeling; driving behavior; Gaussian mixture model (GMM); pedal operation; spectral analysis

I. INTRODUCTION

Driving is indispensable in daily life. To improve safety and traffic efficiency, intelligent transportation system (ITS) technologies including car navigation systems, electronic toll collection systems, adaptive cruise control (ACC), and lane-keeping assist systems (LKAS) have been developed over the last few decades. ACC and LKAS assist drivers by automatically controlling vehicles using observable driving signals of vehicle status or position, e.g., velocity, following distance, and relative lane position. Other research addressing driving signals includes driving behavior modeling that predicts the future status of a vehicle [1]–[3], drowsy or drunk driving detection with eye monitoring [4], [5], and the cognitive modeling of drivers [6].

Driving behaviors differ among drivers. They differ in how they hit the gas and brake pedals, in the way they turn the steering wheel, and in how much distance they keep when following a vehicle [7], [8]. Consequently, ITS applications are expected to be personalized for different drivers according to individual driving styles. One way to

Manuscript received January 31, 2006; revised June 17, 2006. This work was supported by a grant from the Ministry of Education, Culture, Sports, Science and Technology, Japan for the Center for Integrated Acoustic Information Research (CIAIR) Project of the Center of Excellence (COE) Formation Program.

C. Miyajima, **Y. Nishiwaki**, and **K. Takeda** are with Graduate School of Information Science, Nagoya University, Chikusa-ku, Nagoya 464-8603, Japan (e-mail: miyajima@is.nagoya-u.ac.jp; nisiwaki@sp.m.is.nagoya-u.ac.jp; kazuya.takeda@nagoya-u.jp).

K. Ozawa is with Automotive Electronic Components Company, OMRON Corporation, Aichi 485-0802, Japan (e-mail: ozawa@autos.omron.co.jp).

T. Wakita is with Toyota Central R&D Laboratories, Aichi 480-1192, Japan (e-mail: wakita@mosk.tytlabs.co.jp).

K. Itou is with the Faculty of Computer and Information Sciences, Hosei University, Koganei, Tokyo 184-0002, Japan (e-mail: itou@k.hosei.ac.jp).

F. Itakura is with Department of Information Engineering, Meijo University, 1 Tempaku-ku, Nagoya 468-8502, Japan (e-mail: itakuraf@ccmfs.meijo-u.ac.jp).

Digital Object Identifier: 10.1109/JPROC.2006.888405

achieve this is to assist each driver by controlling a vehicle based on a driver model representing the typical driving patterns of the target driver. Driver models for individual drivers or for subgroups of drivers classified based on their driving styles would be trained either in offline or online mode, and an ITS application would choose a driver model appropriate for assisting the target driver by identifying the driver or finding the model that suits his/her driving style.

In this paper, we model individual differences among drivers, especially in distance-keeping patterns when following a vehicle and in pedal operation patterns while driving [9]–[12]. We also evaluate how well driver models can represent driver characteristics in driver identification experiments. First, the relationship between following distance and velocity for each driver is mapped into a two-dimensional distribution and modeled with an optimal velocity (OV) scheme approximated by a monotonically increasing nonlinear function [13], [14] or a statistical method of a Gaussian mixture model (GMM) [15]. Second, gas and brake pedal operation patterns are modeled with GMMs. The distributions of raw pedal operation signals or spectral features obtained from the raw pedal operation signals are modeled with GMMs. We apply spectral (cepstral) analysis to the gas and brake pedal signals to obtain cepstral coefficients, the most widely used spectral features for speech recognition [16]. A cepstrum is defined as the inverse Fourier transform of the log power spectrum of a signal, which allows us to smooth the structure of the spectrum by keeping only the first several lower order cepstral coefficients and setting the remaining coefficients to zero. Assuming that individual differences in pedal operation patterns while driving can be represented by the smoothed spectral envelope of pedal operation signals, we model the pedal operation patterns of each driver with lower order cepstral coefficients. The driver models are compared and evaluated in driver identification experiments using the driving signals of 12 drivers collected in a driving simulator and 276 drivers collected in a real vehicle on city roads.

The rest of this paper is organized as follows. Section II describes the details of the data collection of driving signals in a driving simulator and in a real vehicle. Section III is devoted to driver modeling based on car-following patterns with the OV model and GMM. Section IV concentrates on driver modeling based on pedal operation patterns with GMMs that reflect the distributions of the raw pedal signals and the spectral features of pedal signals. Finally, Section V concludes the paper with a summary and future work.

II. COLLECTION OF DRIVING SIGNALS

Observable driving signals can be categorized into three groups: 1) driving behavior, e.g., gas and brake pedal pressures and steering angles; 2) vehicle status, e.g., velocity, acceleration, and engine speed; and 3) vehicle position, e.g., following distance, relative lane position, and yaw angle. Among these driving signals, we focus on driving behavior with respect to the relationship between following distance and velocity and gas and brake pedal operation signals.

A. Data Collection in Driving Simulator

A driving simulator, which simulated a two-lane expressway and displayed the view from a driver's seat on an LCD monitor, was used for data collection. Twelve participants including eleven males and one female with driver's licenses drove in the simulator for 20 min in four 5-min segments. They were instructed to follow without passing the vehicle displayed in the monitor. The moving patterns of the lead vehicle were collected in a real environment on a relatively congested expressway in Japan. The same moving patterns of the lead vehicle were used for all drivers. Fig. 1 shows examples of 5-min driving signals collected in the simulator. Fig. 1(a) shows the velocity pattern of the lead vehicle. Driving signals including (b) velocity of the ego vehicle, (c) following distance from the lead vehicle, (d) gas pedal position, and (e) brake pedal position were collected and sampled at 100 Hz. Gas and brake pedal positions were digitized to 0–10 000 and 0–5000 levels, respectively, so that 10 000 or 5000 corresponded to full throttle or completely

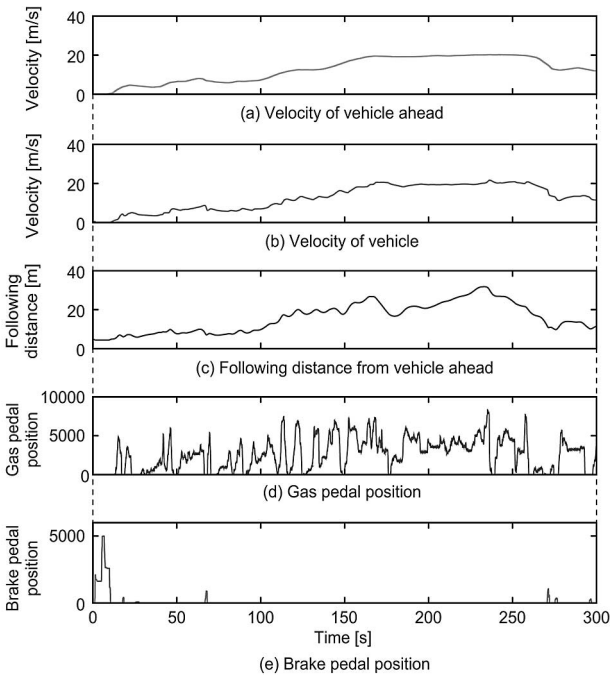

Fig. 1. *Examples of driving behavior signals collected in a driving simulator. (a) Velocity of vehicle ahead; (b) velocity of vehicle; (c) following distance from vehicle ahead; (d) gas pedal position; (e) brake pedal position.*

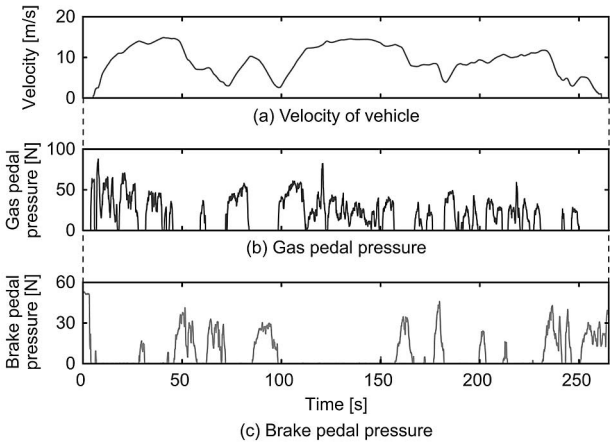

Fig. 2. ***Examples of driving behavior signals collected in a real vehicle. (a) Velocity of vehicle; (b) gas pedal pressure; (c) brake pedal pressure.***

braked positions. Drivers maintained a longer following distance as velocity increased and less frequently pressed the brake pedal while driving on expressways.

B. Data Collection in a Real Vehicle

Driving signals were also collected using a data collection vehicle (Toyota Regius) specially equipped for data collection by the Center for Integrated Acoustic Information Research (CIAIR) Project. The driving data of 276 drivers, including 202 males and 74 females, were used in the experiments. Each driver drove the car on city roads, and five-channel driving signals, 16-channel speech signals, three-channel video signals, and differential GPS were recorded. The driving signals included force on the gas and brake pedals, engine speed, car velocity, and steering angles. These signals were originally sampled at 1 kHz and downsampled at 100 Hz in the experiments. Detailed information on the CIAIR corpus can be found in [17].

Fig. 2 shows examples of driving signals collected in the data collection vehicle. The top, center, and bottom figures correspond to the velocity of the vehicle, gas pedal pressure, and brake pedal pressure, respectively.

Note that the pedal sensors mounted on the real vehicle differ from those mounted on the driving simulator; the pedal sensors of the data collection vehicle recorded the force on the pedals while the driving simulator recorded the gas and brake pedal positions.

III. DRIVER MODELING BASED ON DIFFERENCES OF CAR-FOLLOWING PATTERNS

"Driving behavior" is a cyclic process, as shown in Fig. 3.

1) The driver recognizes the road environment including road layout, traffic conditions, and the behavior of nearby vehicles, e.g., distance from the vehicle in front, and decides actions to take, such as accelerating, braking, and/or steering.
2) The driver operates the gas and brake pedals and the steering wheel.
3) The vehicle status, e.g., velocity and yaw angle, changes based on the driver's operation.
4) The road environment, e.g., distance to the vehicle ahead, changes based on the vehicle status.

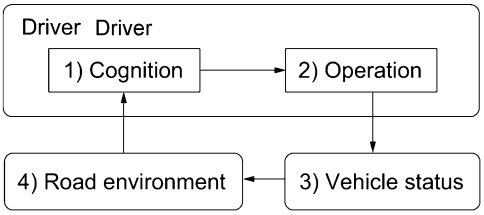

Fig. 3. ***Cyclic process of "driving behavior."***

In this section, we focus on the car following patterns of drivers, which are modeled based on the differences in distance-keeping patterns while following a vehicle. Examples of such trajectories of the relationship between following distance and velocity mapped into a two-dimensional space are shown in Fig. 4. A driver maintains a comfortable time gap to the leading vehicle by adjusting his/her own threshold based on traffic conditions [8]. The trajectories are assumed to represent following distance at each speed with which drivers feel comfortable. Drivers 1 and 3 are more aware of the velocity of the lead vehicle and adjust velocity more frequently in accordance with the following distance. On the other hand, Drivers 2 and 4

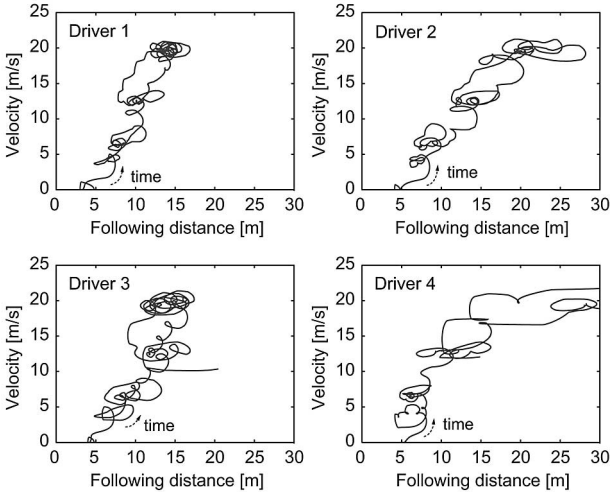

Fig. 4. ***Trajectories of relationship between velocity and following distance for four drivers.***

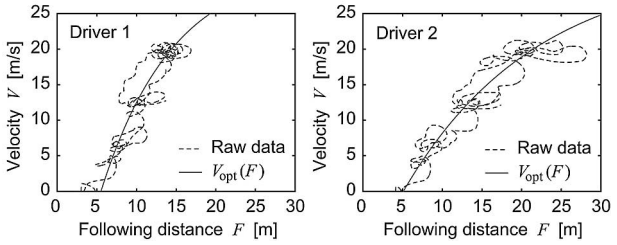

Fig. 5. ***Examples of estimated OV curves for two drivers approximating two-dimensional distribution of following distance and velocity.***

have a horizontal spread of trajectories, i.e., they tend to maintain a constant velocity up to a certain following distance.

A. Modeling With an OV Model

The car-following patterns of each driver were modeled with an OV model, a traffic flow model originally proposed in [13] and [14]. The OV model assumes that drivers have their own OV for a given distance from the vehicle ahead and accelerate or decelerate based on the difference between current velocity $v(t)$ and OV $V_{\mathrm{opt}}(h(t))$

$$\frac{dv(t+\tau)}{dt} = \alpha\{V_{\mathrm{opt}}(h(t)) - v(t)\} \tag{1}$$

where τ is the delay time of the response, α is a sensitivity factor denoting the speed of the response of the driver, and $V_{\mathrm{opt}}(h(t))$ is an OV function of following distance $h(t)$ for which we use a monotonically increasing exponential function

$$V_{\mathrm{opt}}(h(t)) = V_{\max}[1 - \exp\{a(h(t) - h_0)\}] \tag{2}$$

where a and h_0 correspond to the slope and the intercept of the exponential function, respectively, and $V_{\max}$ is the maximum velocity of the vehicle.

Examples of OV functions estimated for two drivers are shown in Fig. 5. For Drivers 1 and 2, $(a, h_0) = (0.11, 5.52)$ and $(a, h_0) = (0.06, 5.10)$ were obtained, respectively, by the least squares method, where 32 m/s for $V_{\max}$ and 500 ms for τ were chosen in a preliminary experiment. Driver 1 has a larger value of a and a steeper slope than Driver 2.

B. Modeling With a GMM

A GMM was then used for modeling driver's car-following patterns. GMM is a statistical model widely used in pattern recognition including speech and speaker recognition [15]. It is defined as a mixture of multivariate Gaussians, and the probability of D-dimensional observation vector $\boldsymbol{o}$ for GMM λ is obtained as follows:

$$b(\boldsymbol{o}|\lambda) = \sum_{i=1}^{M} w_i \mathcal{N}_i(\boldsymbol{o}), \tag{3}$$

where M is the number of the Gaussians of the GMM and $\mathcal{N}_i(\boldsymbol{o})$ is the D-variate Gaussian distribution of the ith component defined with mean vector $\boldsymbol{\mu}_i$ and covariance matrix $\boldsymbol{\Sigma}_i$:

$$\mathcal{N}_i(\boldsymbol{o}) = \frac{1}{\sqrt{(2\pi)^D |\boldsymbol{\Sigma}_i|}} \exp\left\{-\frac{1}{2}(\boldsymbol{o}-\boldsymbol{\mu}_i)' \boldsymbol{\Sigma}_i^{-1} (\boldsymbol{o}-\boldsymbol{\mu}_i)\right\} \tag{4}$$

where $(\cdot)'$ and $(\cdot)^{-1}$ denote transpose and inverse matrices, respectively. w_i is a mixture weight for the ith component and satisfies $\sum_{i=1}^{M} w_i = 1$.

GMM parameters were estimated using the expectation maximization algorithm. Examples of GMMs estimated for two drivers are shown in Fig. 6. The raw signal shown in the same figure was one piece of the data used for training GMMs. GMM can cover the distribution of the trajectories of the raw signal more precisely than the OV model.

C. Comparison of Driver Models Based on OV Model and GMM in Driver Identification

A small driver identification experiment was conducted using a subdata set of eight male drivers collected in the simulator. Three parameters including a, h_0, and α were used as feature vectors for the OV model. Similarity was measured by Mahalanobis distance, and an unknown driver was identified by finding a driver

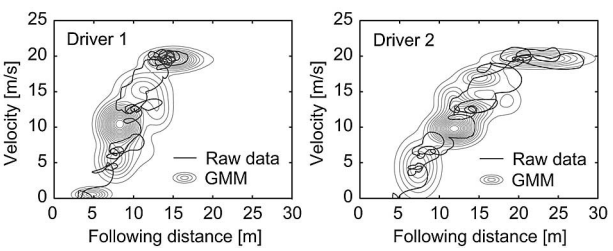

Fig. 6. ***Examples of estimated GMMs for two drivers approximating two-dimensional distribution of following distance and velocity. Each GMM has eight Gaussians with diagonal covariance matrices.***

who had a minimum distance to input data $\boldsymbol{O} = (\boldsymbol{o}(1), \boldsymbol{o}(2), \ldots, \boldsymbol{o}(T))$

$$\hat{k} = \arg\min_{k} \sum_{t=1}^{T} (\boldsymbol{o}(t) - \boldsymbol{\mu}_k)' \boldsymbol{\Sigma}_k (\boldsymbol{o}(t) - \boldsymbol{\mu}_k) \tag{5}$$

where $\boldsymbol{\mu}_k$ and $\boldsymbol{\Sigma}_k$ denote the mean vector and the covariance matrix for driver k.

For GMM driver modeling, an unknown driver was identified as driver $\hat{k}$ who gave the maximum value of the log-likelihood for observation sequence $\boldsymbol{O}$

$$\hat{k} = \arg\max_{k} \log P(\boldsymbol{O}|\lambda_k) \tag{6}$$

$$= \arg\max_{k} \sum_{t=1}^{T} \log b(\boldsymbol{o}(t)|\lambda_k). \tag{7}$$

Each driver drove four times for 5 min each. A four-fold cross-validation approach was used for evaluation. Three of the four driving data were used for modeling each driver, and the excluded data was used as a test. An average driver identification rate was obtained from the four cross-validation tests. The OV model and the GMM were compared, and the GMM driver model gave a better identification rate; 69.0% with GMM and 54.7% with the OV model were obtained for an eight-driver identification task.

Modeling of car-following patterns was conducted only for the simulator because the data collection vehicle did not have distance sensors. We recently mounted distance sensors on a new data collection vehicle and started collecting following distance data in field tests.

IV. DRIVER MODELING BASED ON DIFFERENCES IN PEDAL OPERATION PATTERNS

Pedal operation patterns also differed among drivers. Fig. 7 shows examples of gas pedal operation signals of 150 s collected in the driving simulator for two drivers. They were all recorded with the same moving pattern of a lead vehicle. Pedal operation patterns are similar in the same driver but different between the two drivers.

We modeled the differences in the gas and brake pedal operation patterns with GMMs using the following two kinds of features.

A. Modeling Based on Raw Pedal Operation Signals

Pedal operation patterns can be visualized with histograms of raw pedal operation signals, as shown in Fig. 8. They significantly differ from each other. Driver 1 has a symmetric distribution around 4000, whereas

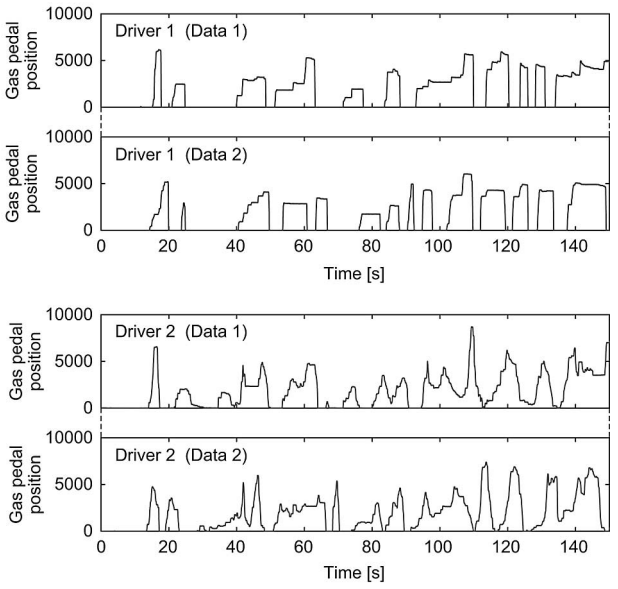

Fig. 7. ***Examples of gas pedal operation patterns for two drivers (top: Driver 1; bottom: Driver 2).***

Driver 2 has a peak around 2000 and a wider spread to the right than to the left. Driver 2 also has a sharp peak near zero because he usually puts his foot on the gas pedal even when not accelerating. Driver 3 has a relatively flat and wide-range distribution. Driver 4 has a similar distribution to Driver 2 but without a sharp peak near zero.

These distributions of raw pedal operation signals were modeled with GMMs. Fig. 9 shows estimated GMMs with eight Gaussians for Drivers 1 and 2, where the histograms are well approximated by GMMs.

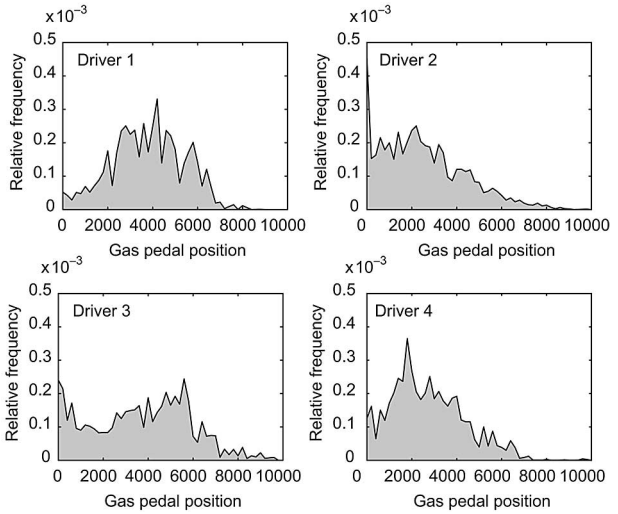

Fig. 8. ***Histograms of gas pedal signals for four drivers.***

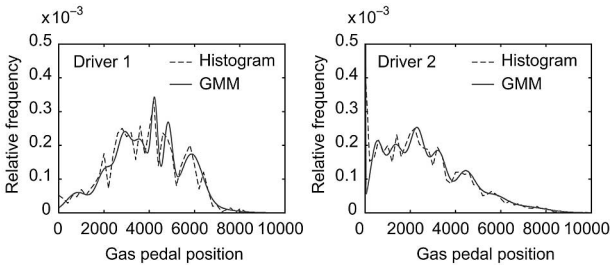

Fig. 9. *Examples of estimated GMMs for two drivers approximating distribution of raw gas pedal signals. Each GMM has eight Gaussians with diagonal covariance matrices.*

B. Modeling Based on Spectral Features of Pedal Operation Signals

Examples of gas pedal operation signals for two drivers are shown in Fig. 10, and their corresponding spectra and spectral envelopes are shown in the center and bottom of the figure, respectively. Each figure shows three examples of 1.28-s-long gas pedal signals. Driver 1 in Fig. 10 (left) accelerates rapidly, while Driver 2 in Fig. 10 (right) tends to gradually increase pressure on the gas pedal. The spectral envelopes shown at the bottom are similar in the same driver but different between the two drivers, which motivated the use of cepstrum (cepstral coefficients) for driver modeling to characterize short-term pedal signals.

Cepstrum is the widely used spectral feature for speech and speaker recognition [16], defined as the inverse Fourier transform of the log power spectrum of the signal. As shown in Fig. 11, cepstral analysis allows us to smooth the structure of the spectrum by keeping only the first several lower order cepstral coefficients and setting the remaining coefficients to zero. Assuming that individual differences in pedal operation patterns can be represented by the smoothed spectral envelope of pedal operation signals, we modeled the pedal operation patterns of each driver with lower order cepstral coefficients.

Speech modeling assumes that vocal cord excitation (vibration), represented by the fine structure of the spectrum, is filtered with the vocal tract represented by the spectral envelope. As shown in Fig. 12, in driver modeling, we assume that command signal for hitting a pedal $e(n)$ is filtered with driver model $H(e^{j\omega})$ represented as the spectral envelope, and the output of the system is observed as pedal signal $x(n)$, e.g., in gas pedal operation, a command signal is generated when a driver decides to hit the gas pedal, and $H(e^{j\omega})$ represents the process of acceleration. This can be described in frequency domain as follows:

$$X(e^{j\omega}) = E(e^{j\omega})H(e^{j\omega}) \tag{8}$$

$$\log|X(e^{j\omega})| = \log|E(e^{j\omega})| + \log|H(e^{j\omega})| \tag{9}$$

where $X(e^{j\omega})$ and $E(e^{j\omega})$ are the Fourier transforms of $x(n)$ and $e(n)$, respectively. We focus on driver characteristics represented as frequency response $H(e^{j\omega})$.

Assuming that the spectral envelope can capture the differences between the characteristics of different drivers, we focused on the differences in spectral envelopes represented by cepstral coefficients (cepstrum), which were also modeled with GMMs.

C. Dynamic Features of Driving Signals

As in speech and speaker recognition, we found that the dynamic features of the driving signals offer much information on driving behaviors. Dynamic features are defined as the following linear regression coefficients:

$$\Delta \boldsymbol{o}(t) = \frac{\sum_{k=-K}^{K} k\boldsymbol{o}(t+k)}{\sum_{k=-K}^{K} k^2} \tag{10}$$

where $\boldsymbol{o}(t)$ is a static feature of raw signals or cepstral coefficients at time t and K is the half window size for

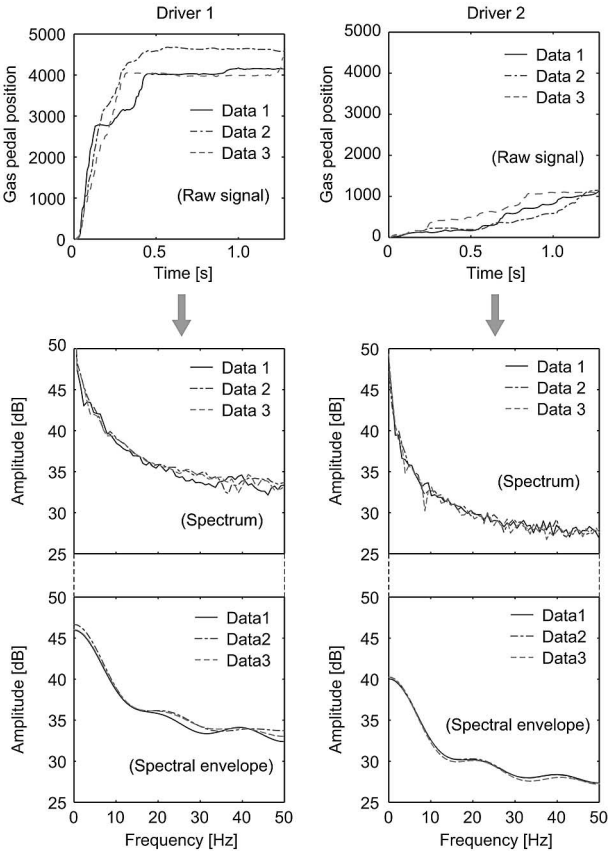

Fig. 10. *Examples of gas pedal operation signals and their spectra for two drivers (left: Driver 1; right: Driver 2).*

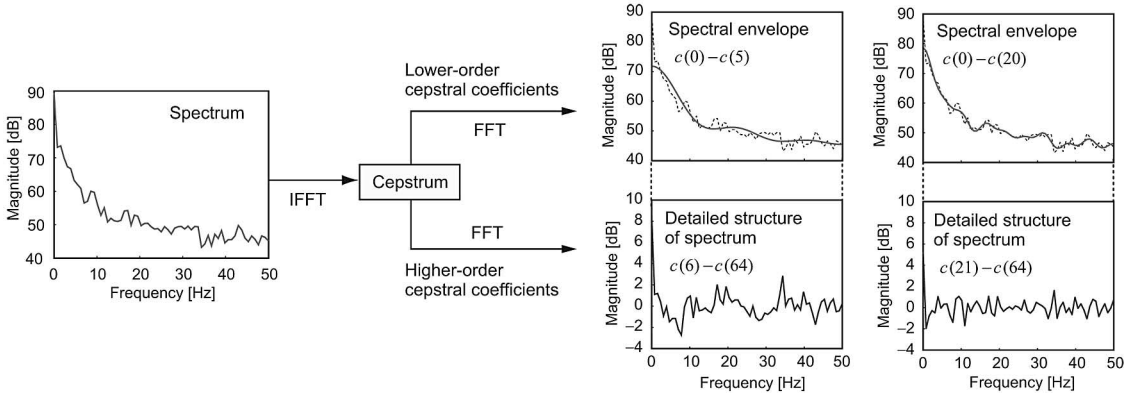

Fig. 11. ***Examples of spectral envelopes extracted through spectral analysis using lower order cepstral coefficients c(0)–c(5) or c(0)–c(20).***

calculating the Δ coefficients. We determined the regression window to be $2K = 800$ ms from preliminary experiments for both raw pedal signals and cepstral coefficients. If $\boldsymbol{o}(t)$ is a D-dimensional vector, D dynamic coefficients are obtained from the static coefficients, combined into a $2D$ dimensional vector, and modeled with GMMs.

D. Driver Identification Experiments in a Driving Simulator

1) Experimental Conditions: Brake pedal signals were not used for driver modeling in the driving simulator experiments because drivers step on the brake pedal less frequently while driving on expressways without traffic signals. Gas pedal operation patterns for each driver were modeled using raw pedal signals or cepstral coefficients obtained from the raw signals and their dynamics calculated as in (10) with a regression window of $2K = 0.8$ s. To obtain cepstral sequences from the pedal signals, 1.28-s frame length and 0.1-s frame shift were chosen for the spectral analysis in preliminary experiments. The feature distributions were modeled using GMMs with 8, 16, or 32 Gaussians and diagonal covariance matrices. Twelve drivers drove four times for 5 min each. A four-fold cross-validation approach was used for evaluation. Three of the four driving data were used for GMM training, and the excluded data was used as a test.

2) Experimental Results: Fig. 13 shows the results for the driver model using raw driving signals. In the figure, velocity, following distance, and gas pedal position are denoted as V, F, and G, and their dynamics as ΔV, ΔF, and ΔG, respectively.

The best performance of a 72.9% identification rate was obtained when using all three signals and their dynamics. Identification performance of the car-following models denoted by the combination of V and F was relatively lower than pedal operation patterns denoted by G, but significantly above the chance level. This result

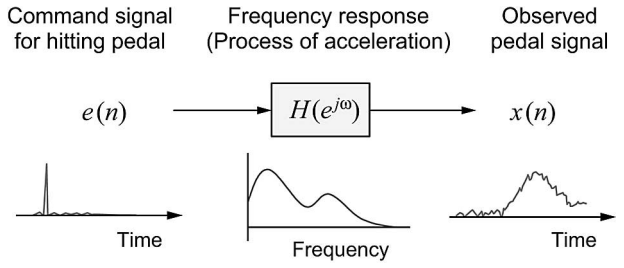

Fig. 12. ***General modeling of driving signals.***

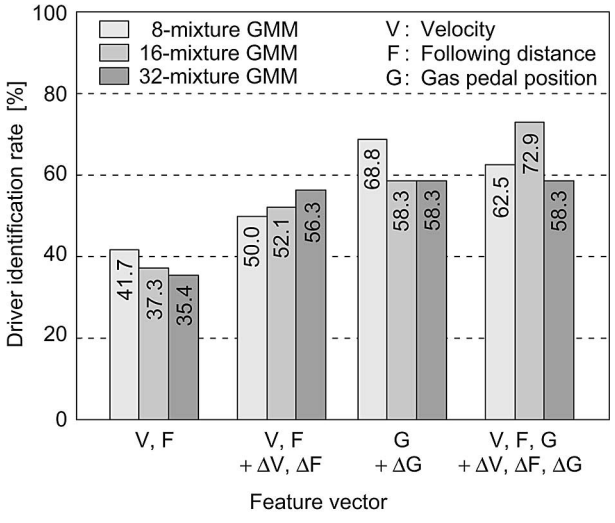

Fig. 13. ***Driver identification rate for GMM driver models using raw driving signals (driving simulator).***

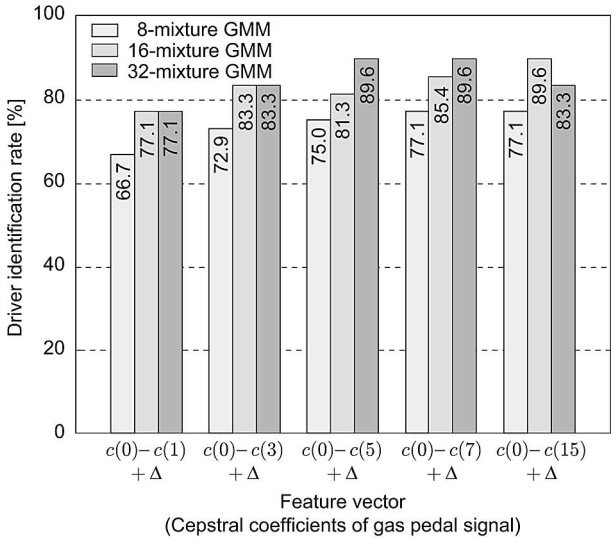

Fig. 14. ***Driver identification rate for GMM driver models using cepstral features (driving simulator).***

indicates that drivers can be classified into groups of driving styles according to their car-following patterns; Fancher *et al.* [7] classified drivers into five categories including flow conformist, extremist, hunter/tailgater, planner, and ultraconservative. Headway control is expected to be personalized based on such categories of driving styles.

Fig. 14 shows the results for the driver model using cepstral coefficients obtained through spectral analysis. In the figure, "$c(0) - c(m)$" represents $m+1$ cepstral coefficients in the lower quefrency range, including from the zeroth to the mth cepstral coefficients. Cepstral features achieved much better performance than raw signals, and an identification rate of 89.6% was obtained. From the experimental results, we confirmed that cepstral features representing the spectral envelope can capture driver characteristics more efficiently than raw driving signals.

E. Driver Identification Experiments in a Real Vehicle

1) Experimental Conditions: The driving data of 276 drivers collected on city roads in the data collection vehicle were used, excluding data collected while not moving. Driving signals of 3 min were used for GMM training and another 3 min for testing. We used brake pedal signals as well as gas pedal signals in the real vehicle experiments because drivers use the brake pedal more often during city than expressway driving.

Cepstral coefficients obtained from the brake pedal signals are also modeled with a GMM, and their log-likelihood was linearly combined with that of a GMM for the gas pedal signals. In driver identification, the unknown driver was identified as driver $\hat{k}$ who gave the maximum weighted GMM log-likelihood over the gas and brake pedals

$$\hat{k} = \arg\max_{k} \left\{ \gamma \log P(\boldsymbol{G}|\lambda_{G,k}) + (1-\gamma) \log P(\boldsymbol{B}|\lambda_{B,k}) \right\} \quad 0 \le \gamma \le 1 \quad (11)$$

where $\boldsymbol{G}$ and $\boldsymbol{B}$ are the cepstral sequences of the gas and brake pedals and $\lambda_{G,k}$ and $\lambda_{B,k}$ are the kth driver models of the gas and brake pedals, respectively. $\gamma (0 \le \gamma \le 1)$ is a linear combination weight for the log-likelihood of gas pedal signals.

2) Experimental Results: As described in Section II-B, the pedal sensors mounted on the real vehicle differ from those mounted on the driving simulator, and a 0.32-s frame length was chosen for the spectral analysis of pedal pressures of the real vehicle, and a 1.28-s frame length for the simulator. Examples of gas pedal operation signals for two drivers collected in the real vehicle are shown in Fig. 15 (top), and their corresponding spectra are shown in Fig. 15 (bottom). Each figure shows three examples of 0.32-s gas pedal signals. Driver A in Fig. 15 (left) tends to gradually increase pressure on the gas pedal, whereas Driver B in Fig. 15 (bottom) accelerates in two stages. After initial acceleration, Driver B momentarily reduces pressure on the gas pedal and then resumes acceleration. The spectra shown in the bottom figures are similar in the same driver but different between two drivers.

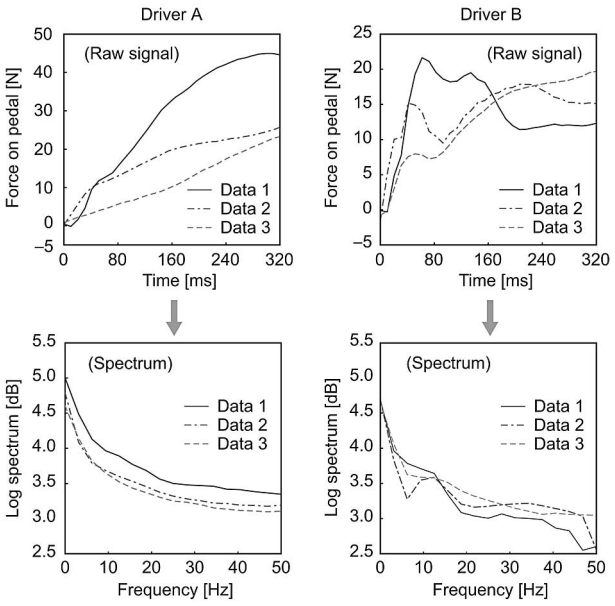

Fig. 15. ***Examples of gas pedal operation signals and their spectra for two drivers (left: Driver A; right: Driver B).***

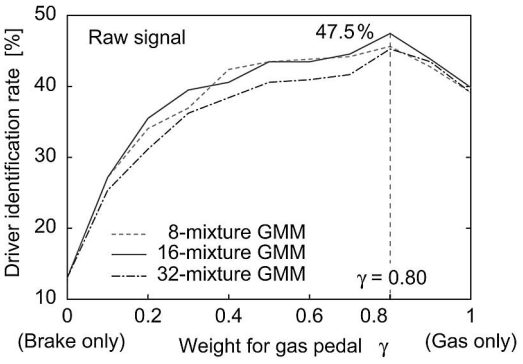

Fig. 16. *Results for combination of gas and brake pedals (raw signals).*

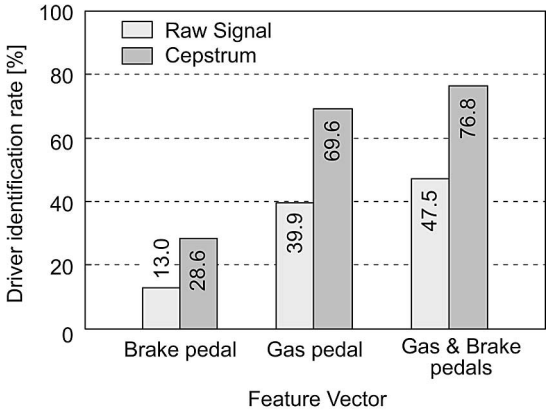

Fig. 18. *Comparison of identification rates for raw pedal signals and cepstral coefficients (field test).*

Figs. 16 and 17 show identification results for the gas and brake pedal signals collected in a real vehicle when using raw signals and cepstral coefficients (cepstrum), respectively. The leftmost results correspond to the identification rates when only using the brake pedal signals, and the rightmost results were obtained with gas pedal signals alone. The gas pedal signals gave better performance than the brake pedal signals because drivers hit the gas pedal more frequently than the brake pedal, as shown in Fig. 2.

The results for the 16-component GMMs in Figs. 16 and 17 are summarized in Fig. 18. The identification performance was rather low when using raw driving signals: the best identification rate for raw signals was 47.5% with $\alpha = 0.80$. By applying cepstral analysis, however, the identification rate increased to 76.8% with $\alpha = 0.76$. Although the pedal sensors were different from those of the driving simulator, similar results were obtained. We thus conclude that cepstral features captured the individualities of driving behavior better than raw driving signals and achieved better performance in driver identification.

3) Experiments With Different Test Lengths: We investigated the identification performance for different test lengths. Fig. 19 shows the identification rates when changing the test data length to 1, 1.5, and 3 min. Although the identification rate for cepstral features deteriorated to 59.5% with the 1-min test data, it still outperformed the identification rate of raw signals with the 3-min test data.

V. CONCLUSION

In this paper, driver characteristics in car-following and pedal operation patterns were modeled. The former were represented by the relationship between following distance and velocity and modeled for each driver with an OV model or with a GMM. Gas and brake pedal operation patterns were modeled with GMMs that represented the distributions of raw pedal operation signals or spectral characteristics extracted through spectral analysis of the raw pedal operation signals. Driver models were evaluated

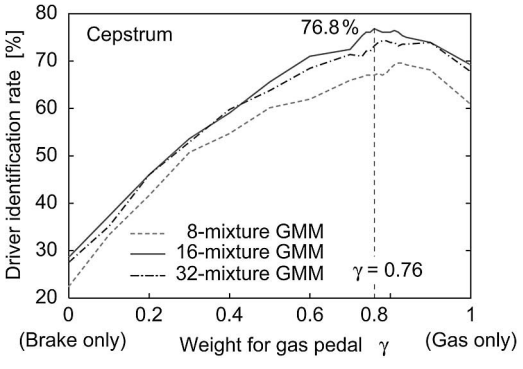

Fig. 17. *Results for combination of gas and brake pedals (cepstrum).*

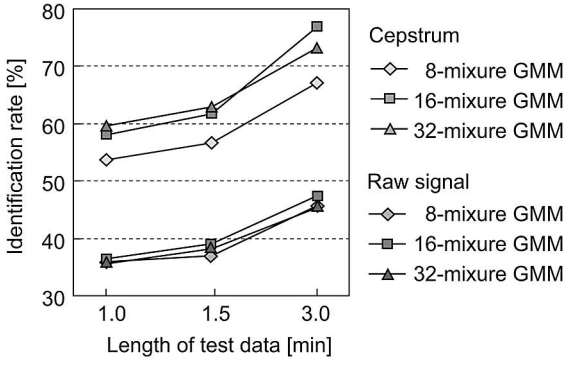

Fig. 19. *Results for different test lengths (field test).*

in driver identification experiments using driving signals collected in a driving simulator and a real vehicle.

Spectral features of pedal signals efficiently modeled driver characteristics and achieved an identification rate of 89.6% for a driving simulator and 76.8% for a field test with 276 drivers, resulting in 61% and 55% error reduction, respectively, over a driver model based on raw pedal operation signals without spectral analysis. Driver identification performance of the car-following models was relatively low compared with the pedal-operation models but significantly above the chance levels. This indicates that drivers can be classified into groups based on their car-following pattens and a driver can be assisted based on the model of the group he/she belongs to.

The selective use of driving signals while accelerating or decelerating and the modeling of characteristics in longer-term driving signals (e.g., more than a 2-s frame length) must be addressed in future work. Other driver modeling techniques apart from GMM, such as hidden Markov models, could be employed for more efficient modeling of the time series of feature vectors. We also plan to use statistical driver models to intelligently assist individual drivers by personalizing headway control to reflect the car-following model that suits the target driver and to detect potentially hazardous situations by detecting unusual driving behavior that is outside of the patterns of a baseline driver model trained using normal driving data. ■

Acknowledgment

The authors would like to thank the editor and the anonymous reviewers for their valuable comments and suggestions. The authors would also like to thank Prof. H. Abut of San Diego State University and Prof. J. Hansen of the University of Colorado for their collaboration and helpful discussion.

REFERENCES

[1] A. Pentland and A. Liu, "Modeling and prediction of human behavior," *Neural Comput.*, vol. 11, pp. 229–242, 1999.

[2] N. Oliver and A. P. Pentland, "Driver behavior recognition and prediction in a SmartCar," in *Proc. SPIE Aerosense 2000, Enhanced and Synthetic Vision*, vol. 4023, pp. 280–290, Apr. 2000.

[3] I. Dagli, M. Brost, and G. Breuel, "Action recognition and prediction for driver assistance systems using dynamic belief networks," in *Lecture Notes in Computer Science*. New York: Springer-Verlag, Oct. 2002, vol. 2592, pp. 179–194.

[4] R. Grace, V. E. Byrne, D. M. Bierman, J. Legrand, D. Gricourt, B. K. Davis, J. J. Staszewski, and B. Carnahan, "A drowsy driver detection system for heavy vehicles," in *Proc. 17th Digital Avionics Systems Conf.*, Oct. 1998, pp. I36/1–I36/8.

[5] P. Smith, M. Shah, and N. D. V. Lobo, "Monitoring head/eye motion for driver alertness with one camera," in *Proc. ICPR 2000*, Sep. 2000, vol. 4, pp. 636–642.

[6] D. D. Salvucci, E. P. Boer, and A. Liu, *Toward an Integrated Model of Driver Behavior in a Cognitive Architecture*, Transportation Research Record, 2001.

[7] P. Fancher, R. Ervin, J. Sayer, M. Hagan, S. Bogard, Z. Bareket, M. Mefford, and J. Haugen, *Intelligent Cruise Control Field Operational Test*, DOT HS 808 849, 1998.

[8] H. Ohta, "Individual differences in driving distance headway," in *Vision in Vehicles: IV*. Amsterdam: North Holland, 1993, pp. 91–100.

[9] K. Igarashi, C. Miyajima, K. Itou, K. Takeda, and F. Itakura, "Biometric identification using driving behavioral signals," in *Proc. ICME 2004*, vol. 1, pp. 65–68, Jun. 2004.

[10] T. Wakita, K. Ozawa, C. Miyajima, and K. Takeda, "Parametric versus non-parametric models of driving behavior signals for driver identification," in *Proc. AVBPA 2005*, pp. 739–747, Jul. 2005.

[11] K. Ozawa, T. Wakita, C. Miyajima, K. Itou, and K. Takeda, "Modeling of individualities in driving through spectral analysis of behavioral signals," in *Proc. ISSPA 2005*, pp. 851–854, Aug. 2005.

[12] C. Miyajima, Y. Nishiwaki, K. Ozawa, T. Wakita, K. Itou, and K. Takeda, "Cepstral analysis of driving behavioral signals for driver identification," in *Proc. ICASSP 2006*, May 2006, vol. 5, pp. 921–924.

[13] M. Brackstone and M. McDonald, "Car-following: A historical review," *Transformation Res.*, pt. F, vol. 2, no. 4, pp. 181–196, Dec. 1999.

[14] M. Bando, K. Hasebe, A. Nakayama, A. Shibata, and Y. Sugiyama, "Dynamical model of traffic congestion and numerical simulation," *Phys. Rev. E*, vol. 51, no. 2, pp. 1035–1042, Feb. 1995.

[15] D. A. Reynolds and R. C. Rose, "Robust text-independent speaker identification using Gaussian mixture speaker models," *IEEE Trans. Speech Audio Process.*, vol. 3, no. 1, pp. 72–83, Jan. 1995.

[16] L. Rabiner and B. Juang, *Fundamentals of Speech Recognition*. Englewood Cliffs, NJ: Prentice-Hall, Apr. 1993.

[17] N. Kawaguchi, S. Matsubara, K. Takeda, and F. Itakura, "Multimedia data collection of in-car speech communication," in *Proc. EUROSPEECH 2001*, Sep. 2001, pp. 2027–2030.

ABOUT THE AUTHORS

Chiyomi Miyajima (Member, IEEE) received the B.E. degree in computer science and the M.E. and Doctorate degrees in electrical and computer engineering from the Nagoya Institute of Technology, Japan, in 1996, 1998, and 2001, respectively.

From 2001 to 2003, she was a Research Associate with the Department of Computer Science, Nagoya Institute of Technology. Currently she is an Assistant Professor with the Graduate School of Information Science, Nagoya University, Japan. Her research interests include speaker recognition, multimodal speech recognition, sign language recognition, and modeling of human behavior.

Yoshihiro Nishiwaki received the B.E. degree from Nagoya University, Japan, in 2005. He is currently pursuing the Master's degree at the Graduate School of Information Science at Nagoya University.

His research mainly focuses on driver modeling for driver assistance systems.

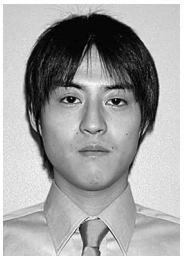

Koji Ozawa received the B.E. and M.E. degrees from Nagoya University, Japan, in 2004 and 2006, respectively.

He is currently with the Automotive Electronic Components Company, OMRON Corporation, Japan. His research interests include the signal processing of driving behavior.

Toshihiro Wakita received the B.E. degree from Kyoto University, Japan, in 1983, the M.S. degree from Tokyo University, Japan, in 1985, and the Ph.D degree in information science from Nagoya University, Japan, in 2006.

Since 1985, he has been with Toyota Central R&D Laboratories, Japan, involved in research on the sound quality of vehicle noise, speech dialogue systems in vehicles, and human interfaces for drivers. He is currently a Research Manager of the Human Factor Laboratory at Toyota Central R&D Laboratories.

Katsunobu Itou received the B.E. and M.E. degrees and the Ph.D degree in computer science from the Tokyo Institute of Technology, Japan, in 1988, 1990, and 1993, respectively.

He then worked at the National Institute of Advanced Industrial Science and Technology (AIST), Tukuba, Japan, as a Senior Research Scientist. From 2003 to 2006, he was an Associate Professor at the Graduate School of Information Science of Nagoya University, Japan. He is currently a Professor at the Faculty of Computer and Information Sciences, Hosei University, Tokyo, Japan. His research interest is in spoken language processing.

Kazuya Takeda (Member, IEEE) received the B.E., M.E., and Doctor of Engineering degrees from Nagoya University in 1983, 1985, and 1994, respectively.

In 1986, he joined the Advanced Telecommunication Research Laboratories (ATR), Kyoto, Japan, where he was involved in two major projects: speech database construction and speech synthesis system development. In 1989, he moved to KDD R&D Laboratories, Japan, and participated in the construction of voice-activated telephone extension systems. Since 1995, he has been working for Nagoya University, Japan. He was a leader of the speech recognition group at the Center for Integrated Acoustic Information Research (CIAIR).

Fumitada Itakura (Fellow, IEEE) received undergraduate and graduate degrees from Nagoya University, Japan. He received the Ph.D. degree in speech processing in 1972.

He joined NTT, Tokyo, Japan, in 1968. He worked at Bell Labs from 1973 to 1975. Between 1975 and 1981, he worked on speech analysis and synthesis based on the Line Spectrum Pair (LSP) method. In 1981, he was appointed chief of the Speech and Acoustics Research Section at NTT. He left in 1984 to take a professorship at Nagoya University. Currently he is a Professor of Meijo University, Nagoya, Japan. His major contributions include theoretical advances involving the application of stationary stochastic processes, linear prediction, and maximum likelihood classification to speech recognition. He patented the PARCOR vocoder in 1969 and the LSP in 1977.

Dr. Itakura's awards include the IEEE ASSP Senior Award in 1975, an award from Japan's Ministry of Science and Technology in 1977, the Morris N. Liebmann Award in 1986, the IEEE Signal Processing Society Award in 1996, the IEEE Third Millennium Medal in 2000, and the Medal with Purple Ribbon from the Japanese Government in 2003. He is a fellow of the Institute of Electronics and Communication Engineers of Japan.